Journal of Power Sources 272 (2014) 190–195

Contents lists available at ScienceDirect

Journal of Power Sources

journal homepage: www.elsevier.com/locate/jpowsour

Ionic conductivity studies of LiBOB-doped silyl solvent blend electrolytes for lithium-ion battery applications

Wilfried V. Barth [a], Adrian Peña Hueso [b,1], Liu Zhou [b,1], Leslie J. Lyons [a,*], Robert West [b,1]

[a] Grinnell College, Department of Chemistry, 1115 8th Ave., Grinnell, IA 50112, USA
[b] Silatronix, Inc., 3587 Anderson Street, Suite 108, Madison, WI 53704, USA

HIGHLIGHTS

- LiBOB/silyl solvent blend electrolytes achieve high ionic conductivities.
- Conductivities are optimized at 0.8 M LiBOB and equal volumes of two silyl solvents.
- Electrolyte conductivities meet the threshold required for commercial application.
- LiBOB/silyl solvent blend electrolytes are stable to 4.6 V vs. Li/Li^+.
- LiBOB/blend electrolytes achieve higher conductivities than pure silyl electrolytes.

ARTICLE INFO

Article history:
Received 18 April 2014
Received in revised form
14 August 2014
Accepted 18 August 2014
Available online 28 August 2014

Keywords:
Lithium-ion batteries
Lithium bis(oxalato)borate
Organosilicon electrolyte
Electrolyte solvent blend

ABSTRACT

The ionic conductivity of LiBOB-doped electrolytes containing two silyl solvents, bis[2-(2-methoxyethoxy)ethoxy] dimethylsilane, **1**, and [2-(2-methoxyethoxy)ethoxy] trimethylsilane,**2**, was measured from −10 °C to 50 °C using AC impedance spectroscopy to assess their potential use in commercial Li-ion cells. The effects of salt concentration, solvent composition, and temperature on the conductivity of the electrolytes are reported. In addition, conductivity data were fit using the Vogel-Tamman-Fulcher (VTF) equation to obtain the parameters σ_0, T_0, and E_a, which correspond closely to conductivity and viscosity. All the electrolytes produced conductivities above the 1.0 mS cm^{-1} threshold required for commercial application. The 1:1 (vl) solvent composition possesses the highest conductivity, with the optimal 0.8 M salt-loading yielding the highest σ_{25} at 1.99 ± 0.02 mS cm^{-1}.
© 2014 Elsevier B.V. All rights reserved.

1. Introduction

Lithium-ion batteries are used in several consumer electronic devices including laptops, cell phones, camcorders, MP3 players and others. More recently, lithium-ion batteries have also found their place in hybrid/electric vehicles and have potential application in renewable energy power plants. However, further improvements in safety, cost, and energy density must be made to meet the performance standards required by hybrid/electric vehicles and renewable energy power plants [1].

Current commercial lithium ion batteries utilize an electrolyte composed of lithium hexafluorophosphate ($LiPF_6$) dissolved in a mixture of ethylene carbonate (EC) and linear esters such as dimethyl carbonate (DMC), diethyl carbonate (DEC), and ethyl methyl carbonate (EMC). The components of these batteries possess several undesirable characteristics. LiPF6 is not stable at higher temperatures and decomposes into LiF and PF_5. PF_5 and $LiPF_6$ also react with water to form HF. These unwanted products contribute to reactions on the electrode surfaces that ultimately result in cell capacity fade and compromise the safety of the cell [2,3]. In addition, the carbonates and esters used in commercial lithium-ion batteries are flammable and potentially toxic [4]. All of the aforementioned issues limit their application in future lithium-ion batteries.

For several years, our group has been developing organosilicon-based electrolytes utilizing siloxanes containing oligo(ethylene oxide) groups. Previous research in our group began with polymer electrolytes utilizing monocomb polysilane polymers with lithium triflate as the salt [5]. This was followed by studies on double-comb polysilane polymers with lithium bis-((trifluoromethyl)sulfonyl) amide (LiTFSA) [6]. Later, even tri and tetra siloxanes with a new

* Corresponding author. Tel.: +1 641 269 3159.
E-mail addresses: info@silatronix.com (A. Peña Hueso), info@silatronix.com (L. Zhou), lyons@grinnell.edu (L.J. Lyons), info@silatronix.com (R. West).
[1] Tel.: +1 608 467 5626.

http://dx.doi.org/10.1016/j.jpowsour.2014.08.075
0378-7753/© 2014 Elsevier B.V. All rights reserved.

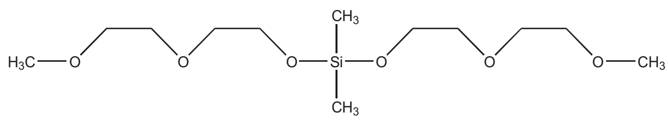

Fig. 1. bis[2-(2-methoxyethoxy)ethoxy] dimethylsilane, **1**,Silyl Solvent. ε = 6.38. η = 3.48. EO/molecule = 4. LiBOB soluble to 1.4 M [31].

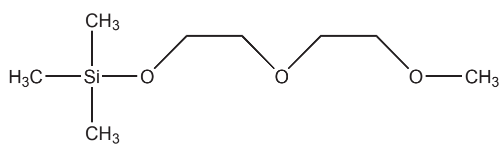

Fig. 2. [2-(2-methoxyethoxy)ethoxy] trimethylsilane,**2**, Silyl Solvent. ε = 4.68. η = 0.90. EO/molecule = 2. LiBOB insoluble [31].

lithium salt, lithium bis(oxalato)borate (LiBOB), were studied [7]. A trend of in-creasing conductivity coupled with low glass transition temperatures, low viscosity, and adequate dielectric constants emerged from these studies, leading to a more recent study with silyl oligoethers with shorter ethylene oxide chains. This study produced some of the highest conducting electrolytes yet, particularly the electrolyte using **2**, which has a σ_{25} of 2.5 mS cm^{-1} [8]. These organosilicon-based electrolytes possess several advantages over current commercial electrolytes. They are nonvolatile, nontoxic, nonflammable, and biocompatible. They also possess low glass transition temperatures and high free volumes, which promote conductivity [4]. In addition, the results of a computational study of these silyl solvents indicate that the Si–O group of these silyl solvents provides added stability for siloxanes in comparison to their carbon analogs [9].

Recently, there has been increased interest in a new promising lithium salt, LiBOB. Previously used salts such as $LiClO_4$, $LiAsF_6$, $LiBF_4$, $LiCF_3 SO_3$, and $LiN(SO_2 CF_3)_2$ have several undesirable characteristics that prevent their use in commercial lithium-ion batteries. For example, $LiClO_4$ has explosion risks associated with $ClO_4^- \cdot AsF_6^-$ is toxic. $LiBF_4$ has low conductivity, and $LiCF_3 SO_3$ and $LiN(SO_2 CF_3)_2$ have the problem of aluminum current-collector corrosion. LiBOB possesses several advantages over previous lithium salts including higher thermal stability (up to 575 K), the ability to passivate aluminum, the formation of a solid electrolyte interface (SEI) on graphite without the presence of ethylene carbonate, and displays higher stability against water [2,10–15]. More recently, LiBOB has found applications in sulfur-based high temperature lithium ion batteries, polymer gel electrolytes, lithium-air batteries, and supercapacitors [16–22].

Previous studies on LiBOB-doped electrolytes have evaluated the salt's use primarily in carbonates such as propylene carbonate (PC), ethylene carbonate (EC), ethyl methyl carbonate (EMC), diethyl carbonate (DEC), ethyl acetate (EA), and γ-butyrolactone (GBL), as well as binary and ternary blends of these carbonates [2,3,23–27]. Typically in commercial batteries, solvents are blended to obtain an optimum set of properties that promote conductivity including low viscosity (η), a high dielectric constant (E), and solvation of the lithium salt [28]. The current study focuses on optimizing LiBOB-doped solvent blends of bis[2-(2-methoxyethoxy)ethoxy] dimethylsilane, **1**, (Fig. 1) and [2-(2-methoxyethoxy)ethoxy] trimethylsilane,**2**, (Fig. 2) molecules, both of which are synthesized by Silatronix, Inc. [29] In our study, **2** is added to **1** to lower viscosity. Simultaneously, **1** will perform the role of solvating LiBOB, which is known to be insoluble in solvents with low dielectric constants and low viscosities, including **2**.

2. Experimental

*2.1. Synthesis of bis[2-(2-methoxyethoxy)ethoxy] dimethylsilane, **1**, and [2-(2-methoxyethoxy)ethoxy] trimethylsilane,**2***

2.1.1. Reagents

Diethylene glycol monomethyl ether, aluminum phosphate monobasic and sodium metal were purchased from Sigma–Aldrich, 1,1,3,3,5,5-hexamethylcyclotrisilazane and 1,1,1,3,3,3-hexamethyl disilazane were pur-chased from Gelest and used without further purification.

*2.1.2. Synthesis of bis[2-(2-methoxyethoxy)ethoxy] dimethylsilane, **1***

Diethylene glycol methyl ether (720 mL, 6.11 mol, 735 g) and hexamethylcyclotrisilazane (245 mL, 1.03 mol, 226 g), were mixed in a 2 L flask at r.t., and aluminum phosphate monobasic (12.5 g, 37 mmol) was added under vigorous stirring. The mixture was slowly heated and kept at 120 °C for 1 h and then heated to 140 °C overnight. The crude product was purified by fractional distillation under reduced pressure (135 °C at 0.4 Torr). It was then dried overnight with molten sodium at 110 °C and distilled again. Final yield: 800 g, 2.70 mol, 88%. δ_H (300 MHz; $CDCl_3$; Me_4 Si) 0.13 (6H, s, Me_2 Si), 3.36 (3H, s, OMe), 3.82, 3.57, 3.63, 3.52 (16H, m, $SiOCH_2$ CH_2 OCH_2 CH_2) in that order.

*2.1.3. Synthesis of [2-(2-methoxyethoxy)ethoxy] trimethylsilane,**2***

Diethylene glycol methyl ether (250 mL, 2.13 mol, 256 g) and hexamethyldisilazane (241 mL, 1.16 mol, 186 g), were mixed in a 1 L flask at r.t. and aluminum phosphate monobasic (10 g, 30 mmol) was added under vigorous stirring. The mixture was slowly heated and kept at 120 °C for 2 h. The crude product was purified by fractional distillation under reduced pressure (50 °C at 0.4 Torr). It was then dried overnight with molten sodium at 110 °C and distilled again. Final yield: 370 g, 1.93 mol, 90%. δ_H (300 MHz;

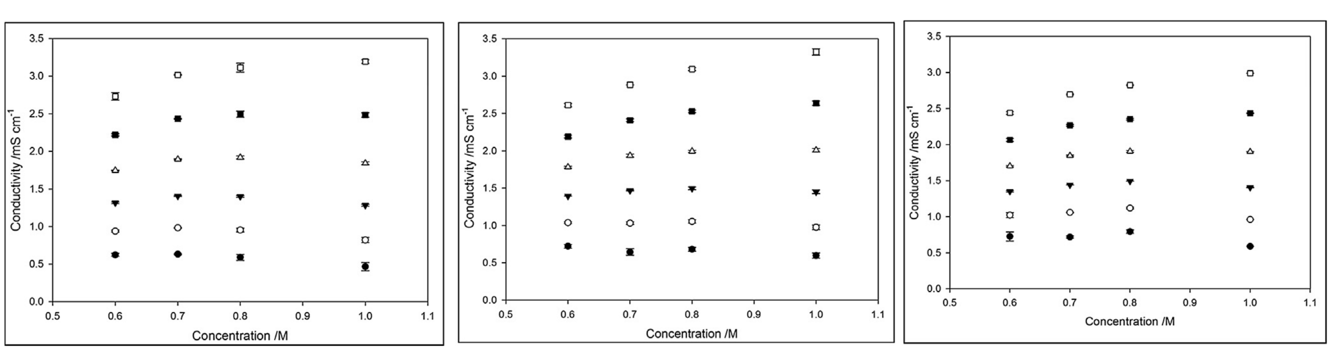

Fig. 3. Change in conductivity (κ) with concentration (M) for a) 3:1,b) 1:1, and c) 1:3 **1**:**2** electrolyte at temperatures of −5 (●), 5 (○), 15 (▼), 25 (△), 35 (■)and 45 (□)°C.

$CDCl_3$; Me_4 Si) 0.11 (9H, s, Me_3 Si), 3.37 (6H, s, OMe), 3.74, 3.56, 3.63, 3.53 (8H, m, $SiOCH_2$ CH_2 OCH_2 CH_2) in that order.

2.2. Electrolyte materials

Lithium bis(oxalato)borate (LiBOB) was supplied by Chemetall and dried via a Schlenck line at 60 °C for 48 h. All electrolytes were mixed in Teflon vials and stored in an argon-filled dry box prior to carrying out conductivity experiments.

2.3. Apparatus for ionic conductivity measurements

Electrolytes were transferred to a custom electrochemical cell in argon-filled dry box, and sealed with an o-ring, cap, and clamp. A condenser wrapped in cotton was attached to a circulating Brinkmann RM6 LAUDA ethylene glycol bath regulating cell temperature, which was monitored with an Omega HH22 thermocouple taped directly to the cell. Variable conductivity measurements were conducted in a copper Faraday cage for temperatures ranging between −10 °C and 50 °C. The impedance of cells was measured using a Princeton Applied Research (PAR) potentiostat galvanostat Model 273A and a PAR Model 1025 frequency response detector which applied an AC potential and measured impedance (Z) and phase shift (θ) over a frequency range from 10 to 100,000 Hz. The four lowest θ values and their corresponding impedances were used to calculate an average conductivity (σ) for conductivity experiments and cell calibrations according to the following equations:

$$R = Z\cos(\theta) \tag{1}$$

$$\sigma = 1/R * 1/A \tag{2}$$

The l/A value of the cell, corresponding to the geometric area between electrodes, was measured using a KCl standard solution. One cell was used during this study, and the l/A values over the course of the study ranged from 0.544 ± 0.006 cm^{-1} to 0.564 ± 0.006 cm^{-1}.

2.4. Voltammetric measurements

Cyclic voltammetry of 0.8 M LiBOB in **1**:**2** (1:1, vol.) and 0.80 M LiBOB in **1** were performed on a Bio-Logic VMP 300 electrochemical workstation using a three electrode cell. A glassy carbon electrode (area = 0.20 cm^2) was used as the working electrode while Li metal served as both counter and reference electrodes in the measurements. The cyclic voltammograms were measured between 0 and 5.0 V vs. Li/Li^+ at a scan rate of 10 mV s^{-1}.

3. Results and discussion

3.1. Effect of temperature, salt concentration, and solvent composition on conductivity

In Figs. 3 and 4, conductivity increases with temperature for all mixtures. This can be explained by increased thermal energy at higher temperatures, which increases ion mobility and therefore conductivity. In addition, the Arrhenius plots are slightly curved, which suggests that EO chain segmental motion contributes to conductivity. These trends have been observed in several previous studies on silyl-based electrolytes including one of our group's recent studies, which focused on trimethylsilyl oligo(ethylene oxide) electrolytes including **2** [4,8].

As seen in Fig. 3, conductivity increases with increasing salt concentration, which is due to an increasing number of free ions. After reaching a maximum conductivity, conductivity plateaus or

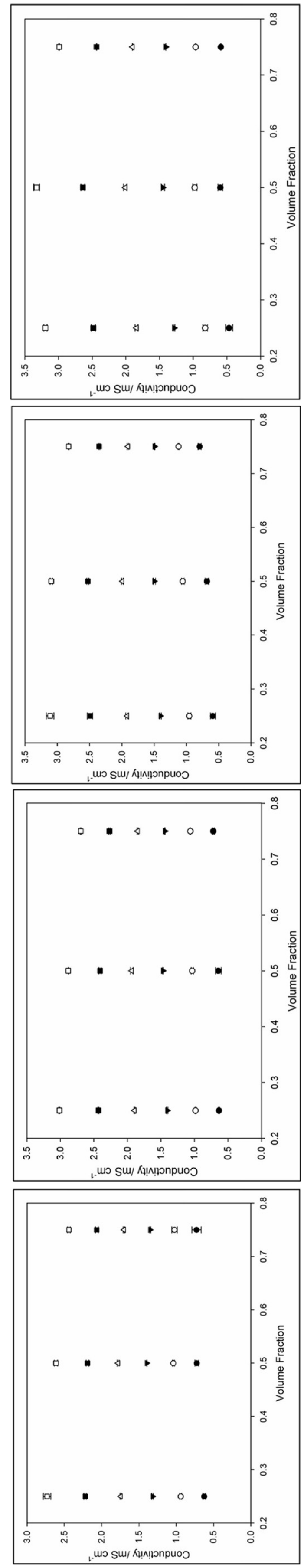

Fig. 4. Change in conductivity (κ) with **2** volume fraction (ϕ) for a) 0.6 M, b) 0.7 M, c) 0.8 M, and d) 1 M concentrations at temperatures of −5 (●), 5 (○), 15 (▼), 25 (△), 35 (■)and 45 (□)°C.

decreases at higher concentrations, which can be attributed to aggregate formation and increased viscosity, which reduces the number and mobility of free ions, respectively [2,28]. Where this peak in conductivity occurs on the axis of concentration depends greatly on the temperature of the electrolyte. At higher temperatures, the peak in conductivity occurs at the maximum concentration (1.0 M), while at lower temperatures it occurs at the minimum concentration (0.6 M). At intermediate temperatures, a peak or plateau in conductivity occurs at 0.8 M. For example, at room temperature (25 °C), conductivity plateaus at ≈2 mS cm^{-1} in both the 1:1 and 1:3 **1**:**2** electrolytes at 0.8 M. In the 3:1 **1**:**2** electrolyte, a peak in conductivity occurs at 0.8 M at room temperature, which indicates that aggregate formation is reduced for the 1:1 and 1:3 blend electrolytes at 1.0 M.

In Fig. 4, the effects of solvent composition (**2**, by volume) on conductivity are much more apparent. At all concentrations it can be seen that as **2** composition is increased, the range in conductivity achieved by the electrolyte narrows. However, despite reduced performance at higher temperatures for high **2** composition, there is increased performance at lower temperatures, which is due to reduced aggregate formation. In attempting to identify an optimum solvent blend, if one looks specifically at the 15, 25, and 35 °C temperatures, a peak in conductivity is observed at the 1:1 **1**:**2** composition across all concentrations. This peak is also seen at 45 °C at 1.0 M. Under these conditions, as **2** composition increases, the initial rise in conductivity can be attributed to falling viscosity, since **2** has a lower viscosity than **1**. After the peak in conductivity is reached, conductivity falls with the decreasing dielectric constant of the solvent blend, leading to increased ion aggregation. The complementary effects of these physical properties have been explored for both the diffusion coefficients and ionic conductivity of mixed carbonate solvent blends in electrolytes of $LiPF_6$. Blending a solvent of lower viscosity with a solvent of higher viscosity increases the diffusion coefficients for both the cation and anion

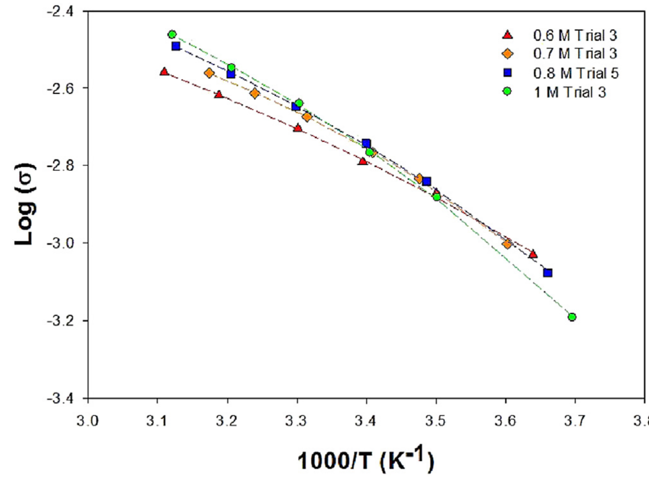

Fig. 6. Arrhenius plot of 1:1 **1**:**2** electrolyte. Only one trial per composition plotted.

while the higher dielectric constant solvent improves ionic conductivity of the blend electrolytes [29]. In general, diffusion coefficients increase in lower viscosity media [30].

Fig. 5 displays 3-D plots of the conductivity data against concentration and solvent composition (**2**, by volume) across the observed range of temperatures. In most of the figures, a “dome” shape can be observed in the plots, which results from conductivity peaking in both concentration and solvent composition for reasons described previously, thus achieving an optimum viscosity and dielectric constant. At lower temperatures where ion mobility is impeded due to ion aggregation, conductivity peaks at low salt concentration and high **2** composition. Decreasing viscosity is increasingly important in impeding the formation of these

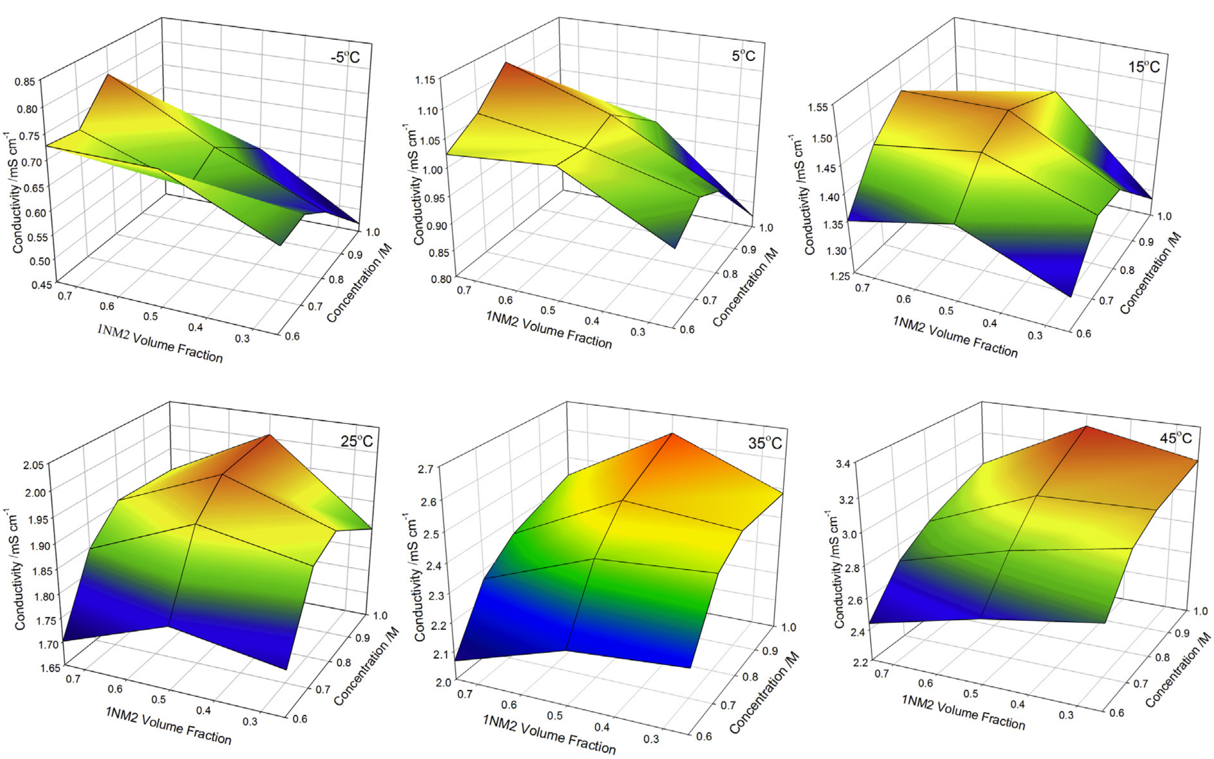

Fig. 5. Change in conductivity (κ) with simultaneous changes in salt concentration (M) and **2** volume fraction (ϕ) at different temperatures for $LiBOB_M\mathbf{1}_{1-\phi}\mathbf{2}_{\phi}$electrolyte. Data plotted was obtained from VTF fits of conductivity data, depicted in Fig. 6.

Table 1
VTF parameters of Arrhenius plots vs. concentration (M) and **2** volume composition (3:1, 1:1, and 1:3 **1**:**2**).

Concentration (M)	σ_{25} (mS cm^{-1})			σ_0 (mS cm^{-1})			E_a (kJ mol^{-1})			T_0 (K)		
	3:1	1:1	1:3	3:1	1:1	1:3	3:1	1:1	1:3	3:1	1:1	1:3
0.60	1.74	1.79	1.71	40 ± 10	30 ± 10	16 ± 1	3.2 ± 0.6	2.9 ± 0.9	1.9 ± 0.2	17_4 ± 11	17_2 ± 20	196 ± 4
0.70	1.89	1.92	1.84	70 ± 20	14 ± 2	22 ± 3	4.1 ± 0.5	1.4 ± 0.1	2.2 ± 0.3	163 ± 8	216 ± 4	188 ± 7
0.80	1.93	1.98	1.92	59 ± 11	35 ± 10	26 ± 4	3.4 ± 0.4	2.6 ± 0.5	2.5 ± 0.3	178 ± 6	19_0 ± 11	184 ± 7
1.00	1.87	1.98	1.90	36 ± 3	44 ± 10	28 ± 3	2.2 ± 0.1	2.7 ± 0.4	2.2 ± 0.2	209 ± 3	195 ± 8	199 ± 4

aggregates, which simultaneously decreases the number of EO units available to dissolve the salt. As temperature increases, this "dome" shifts from low salt concentration and high **2** composition to high salt concentration and low **2** composition. This shift can be explained by increased thermal energy, which limits aggregate formation. As such, viscosity is no longer a limiting factor, so lowering **2** composition affords more EO units to dissolve more salt, freeing more Li^+ ions to contribute to conductivity.

In assessing these mixtures for commercial application, all of the mixtures possessed conductivity above the 1 mS cm^{-1} commercial requirement. However, the 1 M solvent blends required three months for the salt to dissolve, which limits them for commercial application. More importantly, the conductivity of all of the LiBOB-based 0.8 M **1**:**2** mixtures is greater than the conductivity measured by Koua Xiong for 0.8 M pure **1** (1.71 ± 0.01 mS cm^{-1}) [31]. The electrolyte with a solvent blend of 1:1 **1**:**2** and 0.8 M LiBOB produced the highest σ_{25} of all the mixtures, at 1.99 ± 0.02 mS cm^{-1}. This conductivity is higher than those reported for LiBOB and LiTSFI dissolved in a similar silyl solvent with three ethoxy substituents [8,32].

3.2. Trends in VTF parameters

Conductivity data were fit using the Vogel-Tamman-Fulcher (VTF) equation, with Fig. 6 displaying a sample plot for the 1:1 **1**:**2** electrolyte where the VTF fits are displayed as lines [33–35]:

$$\sigma\left(T\right) = \sigma_0 e^{-\left[\frac{B}{(T-T_0)}\right]} \tag{3}$$

The parameters σ_0, T_0, and E_a ($B = E_a/R$) were then obtained from these fits (Table 1). The σ_0 parameter corresponds to the number of mobile charge carriers in the electrolyte and therefore also conductivity [8]. Across almost all the mixtures, the σ_0 parameter increases with salt loading, which makes sense since an increase in salt concentration should increase the number of mobile charge carriers in the mixture. This trend holds true especially for the 1:3 **1**:**2** mixture, which possesses the smallest errors bars. However, for the 3:1 **1**:**2** mixture, this trend does not hold since the errors for the σ_0 parameters are large. As **2** composition is increased, σ_0 decreases for some salt concentrations. However, once errors are taken into account, no apparent trend can be discerned for σ_0 with changing solvent composition.

The E_a (activation energy) and T_0 (vanishing mobility temperature) parameters correlate with the viscosity of the electrolyte [25,28]. Given the magnitudes of the E_a and T_0 values, the mixtures are not particularly viscous. However, it is very hard to discern trends in E_a and T_0 with changes in salt loading and solvent composition, especially when taking errors into account.

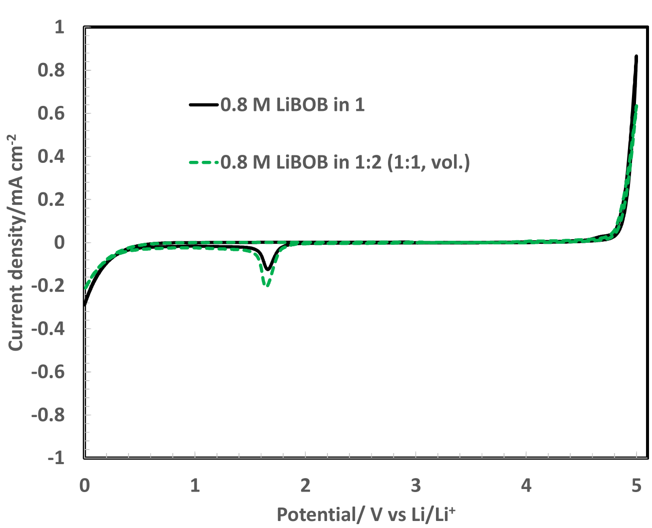

Fig. 7. Cyclic voltammograms of 0.8 M LiBOB in **1** (in solid line), 0.8 M LiBOB in **1:2** (1:1, vol., in dashed line).

3.3. Electrochemical performance

Cyclic voltammetry for the two electrolytes of **1** only with 0.8 M LiBOB and the solvent blend of equal volumes of **1**:**2** and 0.8 M LiBOB are displayed in Fig. 7. In both the single solvent **1** and the mixed solvents the electrolyte is stable to 4.6 V vs. Li/Li^+ which is greater than the upper voltage limit of a disiloxane/LiBOB electrolyte at 4.0 V [36] and similar to the stability (4.4 V) reported for LiBOB in the silyl solvent analogous to **2** with three ethoxy substituents [37] as well as LiBOB in propylene carbonate [38]. The small reduction peak at 1.8 V has been observed before and attributed to products of the LiBOB oxidation [39]. We expect that the flammability of the equal volume blend of **1**:**2** and 0.8 M LiBOB electrolyte will be lower than the carbonate solvents as we have shown previously for other silyl electrolytes [40].

4. Conclusions

LiBOB-based **1**:**2** solvent blends achieved solubility of LiBOB for all electrolyte compositions in this study. The conductivity of the mixtures generally increases with salt concentration because the number of mobile ions in solution promoting conductivity increases. The equal volume **1**:**2** solvent blends exhibited the highest conductivity, suggesting an optimal balance between solvating capability and viscosity was reached. The electrolyte is stable to 4.6 V vs. Li/Li^+ for both the single solvent **1** and the solvent blend. Fitting the VTF equation to conductivity data helped evaluate the parameters σ_0, T_0, and E_a. Conductivity increased with σ_0, corresponding to the increase of mobile ions. No apparent trend was observed for T_0 or E_a.

Acknowledgments

The impedance equipment was acquired with funds provided by the NSF-MRI program (Grant No.0116159).

References

[1] B. Scrosati, J. Solid State Electrochem. 15 (2011) 1623–1630.
[2] F. Azeez, P.S. Fedkiw, J. Power Sources 195 (2010) 7627–7633.
[3] R. Awan, L. Fan, W. Qiu, T. Xing, Ionics 15 (2011) 1623–1630.
[4] N.A. Rossi, R. West, Polym. Int. 58 (2009) 267–272.
[5] L.J. Lyons, B.A. Southworth, D. Stam, R. West, C.-H. Yuan, Solid State Ionics 91 (1996) 169–173.
[6] R. Hooper, L.J. Lyons, M.K. Mapes, D. Schumacher, D.A. Moline, R. West, Macromolecules 34 (2001) 931–936.
[7] K. Amine, L.J. Lyons, K. Morcom, N. Rossi, Y. Schneider, Q. Wang, R. West, Z. Zhang, Chem. Mater. 18 (2006) 1289–1295.
[8] K. Amine, R. Butorac, Z. Chen, S. Harring, L. Lyons, R. West, L. Zhang, Z. Zhang, J. Mater. Chem. 18 (2008) 3713–3717.
[9] K. Amine, R.S. Assary, L.A. Curtiss, P.C. Redfern, Z. Zhang, J. Phys. Chem. 115 (2011) 12216–12223.
[10] L. Larush-Asraf, D. Aurbach, M. Biton, H. Teller, E. Zinigrad, J. Power Sources 174 (2007) 400–407.
[11] Y. An, X. Cheng, C. Du, J. Lin, Y. Ma, G. Yin, P. Zuo, RSC Adv. 2 (2012) 4097–4102.
[12] J.W. Choi, Y.K. Jeong, W. Kim, D.J. Lee, J.-N. Lee, Y.M. Lee, J. Park, M. Ryou, Electrochim. Acta 83 (2012) 259–263.
[13] Y. Akita, K. Dokko, K. Kanamura, M. Matsui, H. Munakata, J. Power Sources 210 (2012) 6–86.
[14] K. Amine, J. Dong, Y. Kusachi, Z. Zhang, J. Phys. Chem. C 115 (2011) 24013–24020.
[15] M. Amereller, J. Barthel, H.J. Gores, J. Lodermeyer, M. Multerer, A. Schmid, C. Schreiner, J. Chem. Eng. Data 54 (2009) 468–471.
[16] Y. Diao, X. Kai, X. Hong, S. Xiong, Ionics 18 (2012) 249–254.
[17] X. Cui, B. Li, S. Li, L. Mao, X. Shi, X. Xu, Y. Zhao, Electrochim. Acta 65 (2012) 221–227.
[18] X. Cui, B. Li, F. Li, S. Li, L. Mao, X. Shi, X. Xu, Electrochim. Acta 79 (2012) 197–201.
[19] S.D. Burton, L. Cosimbescu, M.H. Engelhard, M.E. Gross, E. Nasybulin, W. Xu, J. Zhang, J. Phys. Chem. C 117 (2013) 2635–2645.
[20] K. Edstrom, M. Hahlin, R. Younesi, ACS Appl. Mater. Interfaces 5 (2013) 1333–1341.
[21] S.Z.Z. Abidin, A.M.M. Ali, O.H. Hassan, M.Z.A. Yahya, Int. J. Electrochem. Sci. 8 (2013) 7320–7326.
[22] A. Laheaar, A. Janes, E. Lust, J. Electroanal. Chem. 669 (2012) 67–72.
[23] J. Huang, X. Kang, X. Liu, W. Qiu, T. Xu, Z. Yu, J. Power Sources 189 (2009) 458–461.
[24] M.S. Ding, T.R. Jow, J. Electrochem. Soc. 152 (2005) A1199–A1207.
[25] M.S. Ding, T.R. Jow, K. Xu, J. Electrochem. Soc. 152 (2005) A132–A140.
[26] J. Huang, F. Li, W. Qiu, B. Yu, Int. J. Minerals, Metallurgy Mater. 16 (2009) 463–467.
[27] X.L. Cui, G.X. Li, S.Y. Li, X.M. Shi, X.L. Xu, Russ. J. Electrochem. 48 (2012) 518–524.
[28] M.S. Ding, T.R. Jow, ECS Trans. 16 (2009) 183–214.
[29] K. Hayamizu, J. Chem. Eng. Data 57 (2012) 2012–2017.
[30] K. Hayamizu, Y. Aihara, S. Arai, C.G. Martinez, J. Phys. Chem. B 103 (1999) 519–524.
[31] J. Davis, A.P. Hueso, L.J. Lyons, R. West, K. Xiong, in: 243rd National Meeting of the American Chemical Society, San Diego, CA, 2012. INOR 699.
[32] K. Amine, J. Dong, Y. Kusachi, Z. Zhang, J. Power Sources 196 (2011) 2255–2259.
[33] H. Vogel, Phys. Z 22 (1921) 645.
[34] W. Hesse, G. Tamman, Z. Anorg, Allg. Chern. 156 (1926) 245.
[35] G.S. Fulcher, J. Am. Ceram. Soc. 8 (1925) 339.
[36] Z.C. Zhang, J.A. Dong, R. West, K. Amine, J. Power Sources 195 (2010) 6062–6068.
[37] K. Amine, Q. Wang, D. Vissers, Z. Zhang, N. Rossi, R. West, Electrochem. Commun. 8 (2006) 429–433.
[38] Z.M. Xue, C.Q. Ji, W. Zhou, C.H. Chen, J. Power Sources 195 (2010) 3689–3692.
[39] W. Xu, C.A. Angell, Electrochem. Solid-State Lett. 4 (1) (2001) E1–E4.
[40] L. Zhang, L. Lyons, J. Newhouse, Z. Zhang, M. Straughan, Z. Chen, K. Amine, R.J. Hamers, R. West, J. Mater. Chem. 20 (2010) 8224–8226.